

Soft Matter

Accepted Manuscript



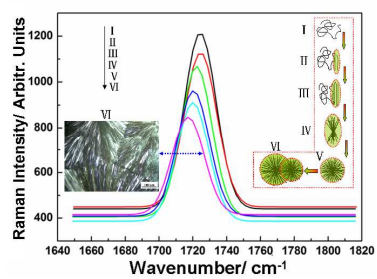
This is an *Accepted Manuscript*, which has been through the Royal Society of Chemistry peer review process and has been accepted for publication.

Accepted Manuscripts are published online shortly after acceptance, before technical editing, formatting and proof reading. Using this free service, authors can make their results available to the community, in citable form, before we publish the edited article. We will replace this *Accepted Manuscript* with the edited and formatted *Advance Article* as soon as it is available.

You can find more information about *Accepted Manuscripts* in the [Information for Authors](#).

Please note that technical editing may introduce minor changes to the text and/or graphics, which may alter content. The journal's standard [Terms & Conditions](#) and the [Ethical guidelines](#) still apply. In no event shall the Royal Society of Chemistry be held responsible for any errors or omissions in this *Accepted Manuscript* or any consequences arising from the use of any information it contains.

A Graphical abstract



Raman shift of C=O bonds reveals the dynamic processes and molecular structural evolution of cold crystallization of amorphous poly(trimethylene terephthalate).



Soft Matter

ARTICLE

Structural Evolution Analysis and Cold-Crystallization Kinetics to Spherical Crystal in Poly (trimethylene terephthalate) Film using Raman Spectroscopy

Received 00th January 20xx,
Accepted 00th January 20xx

DOI: 10.1039/x0xx00000x

www.rsc.org/

Chenglong Hu,^{ab} Shaoyun Chen,^{*a} Weihong Zhang,^c Fangyan Xie,^c Jian Chen^c and Xudong Chen,^b

Dynamic processes and the structural evolution of cold-crystallized poly (trimethylene terephthalate) (PTT) film were investigated using Raman spectroscopy. Raman scattering of C=O stretching vibration was related to the molecular chains movement and structure evolution in PTT during cold crystallization. In particular, the information about each phase of crystallization, including induction, nucleation, nucleus growth, and secondary crystallization, was thoroughly revealed. The experimental results indicated that the kinetics parameters measured by the Raman method were in good agreement with those obtained by differential scanning calorimetry (DSC) and infrared spectroscopy. The blue-shifted C=O stretching vibration resulting from the crystallization process is a popular phenomenon and may therefore have many potential applications in a wide range of areas.

Introduction

With combined physical properties of nylons and other aromatic polyesters providing excellent elastic recovery, poly (trimethylene terephthalate) (PTT) is a potential polymer for various applications, such as engineering plastics and textile fibers.^{1,2} It has also been shown that PTT can be used in the field of optical communications, optical data processing, and nonlinear optics because of its high birefringence and luminous transmittance.³ Although previous studies showed that PTT can crystallize, and that the unit cell in PTT contains two monomer units forming a 2/1 helix, only one crystal form has been identified to date.⁴⁻⁶ As in any material, the macroscopic properties of a polymer are dependent on its molecular structure due to the chemical composition of the material and its response to the myriad of processing conditions. Recently, cold crystallization of PTT has been given considerable attention for its practical use of tailored morphology. For example, in crystalline phase, the conformations of its m-methylene glycol segment are trans-gauche-gauche-trans (tggt) for PTT, all-trans for PET, and either all-trans or gauche-gauche-trans-gauche-gauche (ggtgg)

for PBT.⁷ The degree of crystallinity and development of spherulite are closely related to the mechanical strength of PTT, and the chain deformation of microscopic PTT crystal depends on three methylene units.⁴ Obviously, the chemical composition and molecular conformation play a key role in determining the macroscopic behaviour. Therefore, studying the structural evolution and crystalline kinetics of PTT is important to understand, predict, and design microscopic structures and operational performance under various processing conditions.

So far, several methods have been extensively developed to investigate cold-crystallization behaviour and the morphology of PTT. For example, cold crystallization of PTT has been recently studied by an innovative fluorescence spectroscopy (FL) method because of the specific fluorescence emission of phenylene dimers from adjacent chains of PTT.^{3,8} The three-phase model consisting of crystalline, mobile amorphous, and rigid amorphous phases with structural formation of PTT at various crystallization conditions was illustrated by small angle X-ray scattering (SAXS).⁹ The crystalline behaviour, chain movement, and structure evolution of PTT during cold crystallization were revealed by resonance light scattering (RLS).¹⁰ Also, differential scanning calorimetry (DSC),¹¹ dielectric spectroscopy (DS),¹² infrared spectroscopy (IR)¹³ and atomic force microscopy (AFM)¹⁴ have been used to investigate crystallization of PTT. It is worth noting that the methods discussed above have some shortcomings where cold-crystallization is concerned. The SAXS and DS are not easy to access and the data is difficult to handle. The AFM can only observe the microstructure of material. DSC is not sensitive enough to measure the microscopic vibrations in the molecular skeleton.

^aKey Laboratory of Optoelectronic Chemical Materials and Devices of Ministry of Education, Jiangnan University, Wuhan 430056, China. E-mail: cescsy@jhun.edu.cn (S. Y. Chen)

^bKey Laboratory for Polymeric Composite and Functional Materials of Ministry of Education, DSAPM Lab, School of Chemistry and Chemical Engineering, Sun Yat-sen University, Guangzhou 510275, China.

^cInstrumental Analysis and Research Center, Sun Yat-sen University, Guangzhou 510275, China.

† Footnotes relating to the title and/or authors should appear here. Electronic Supplementary Information (ESI) available: [details of any supplementary information available should be included here]. See DOI: 10.1039/x0xx00000x

In this paper, we demonstrate a nondestructive technique based on the Raman spectroscopy, by which cold-crystallization and structural evolution are evaluated in situ using conventional laboratory equipment. Raman spectroscopy provides information about molecular vibrations, which are sensitive to interactions and conformations of the molecules.¹⁵ However, the Raman scattering signal of strong fluorescent materials can not obtain by Raman spectroscopy because the fluorescence can be excited by laser in match the appropriate excitation wavelength. In addition, Raman scattering signal of the tested material must be strong at low energy excitation by laser due to the telephotolens are used by Raman variable temperature testing. PTT is an intrinsic fluorescent polymer, and its Raman scattering signal is very remarkable excited by 514 nm at telephotolens model. Previous studies reported the crystallization and structure of PTT fiber or film using Raman spectroscopy.^{7, 16, 17} However, processes to gain more detailed information about the molecular structure and orientation of glass transition, crystallization induction phase, nucleation phase, nucleus growth phase, and secondary crystallization phase of amorphous PTT have remained a subject of speculation and controversy.¹⁸ Hereinafter, the present work is committed to explore the Raman spectroscopy method in determining the non-isothermal dynamic process and isothermal cold-crystallization of amorphous PTT film, and to develop a nondestructive and rapid technique for detecting crystallization of the polymer.

Experimental

PTT pellets were provided by Shell Chemicals Co. The intrinsic viscosity is 0.92 dL/g and the melting point is 225 °C. PTT pellets were dried for 48 h under vacuum at 80 °C before use. A glassy amorphous film (about 15 μm thick) was prepared by pressing the pellets under 240 °C for 10 s using Universal Film Maker (0016-010E, Thermo, USA), then rapidly quenching the film in liquid nitrogen.

Raman spectrum measurement was performed on a Renishaw inVia Laser micro-Raman spectrometer (the excitation wavelength was 514 nm). The spectra were typically obtained within 5 s of exposure using telephotolens measurement. The scanning center of the spectrum was 1616 cm⁻¹. Examination of spectra reproducibility and the samples exposed to the laser beam showed that possible damage of the PPT film was avoided. Differential scanning calorimetry (DSC) measurement was performed on a MDSC 2910 (USA) at a heating rate of 5 °C/min in nitrogen. FTIR measurement was performed on a Nicolet/Nexus 670 (USA) at a heating rate of 5 °C/min in air.

Results and discussion

Movement of molecular chains and structural evolution of amorphous PTT during non-isothermal crystallization

Figure 1 shows the Raman spectra obtained on the amorphous and crystalline PTT films. Differences can be observed through the entire spectral range, in accord with the previous available Raman data.⁷ The scattering intensity of the bands at 650, 848, 910, 950 and 1115 cm⁻¹ in crystalline PTT film are remarkably increased compared with that of the amorphous PTT film, whereas the scattering intensity of the band at 1616 cm⁻¹ (ring stretching) obviously decreased, which was caused by limitation of ring stretching vibration.¹⁹ It is worth noting that the band at 1722 cm⁻¹, involved in the C=O symmetric stretching vibration in amorphous PTT, shifted to 1715 cm⁻¹ (shown in the inset of Figure 1) due to the strong dipole-dipole interaction of the C=O bond during crystallization.⁷

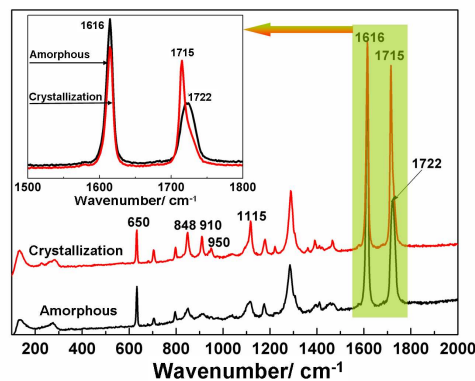


Figure 1 The Raman spectra of amorphous and crystalline PTT film.

Figure 2(a) depicts typical Raman scattering curves of PTT film obtained at certain temperatures after crystallization. The band at 1616 cm⁻¹ is used to study crystallization, and its intensity changes with temperature. Figure 2(b) further shows the temperature dependence of the scattering intensity at 1616 cm⁻¹ within the temperature range of interest. Different stages of macromolecular motions are exhibited by the inflection points on the curve, associated with both relaxation and crystallization during heating. As shown in Figure 2(b), the stage in the temperature region from 38 °C–56 °C is related to the relaxation of PTT chains. In general, orientation relaxation of global chains and relaxation of local molecular chain segments are related to the relaxation of polymeric materials. Because of the tremendous difference between the two scales of movement, the manners in which the two kinds of relaxation follow relaxation regulations are also different. Since amorphous PTT can be assumed to be a homogeneous phase system, and the molecular chain presents in a random coil when PTT chains are frozen by liquid nitrogen quenching from the melting state. At low temperature, the random coil of PTT chains presents in contractile state, which is compelled by the cohesion entanglement between molecules. With increasing of temperature the disentanglement of random coil from contractile state to extend caused by inter-chain cohesive of molecules reducing. The oriented structure of whole polymer chain has been motivated, but did not give rise to the change of Raman intensity at range 38 °C to 42 °C.

With the further increasing of the temperature the local molecular chain segments of PTT start to relax because of the increase of thermal motion energy of the polymer chain. The thermal molecular can overcome the barrier of internal rotation to lead to the relaxation of local molecular bonds and

the conformation of chain segments changed by the internal rotation of the single bond. However, the movement of a whole chain molecule still cannot occur at certain temperatures in this process. As a result, the Raman intensity of the bond at 1616 cm^{-1} decreased sharply at 42 °C – 50 °C , then slowly increased at 50 °C – 56 °C . This was caused by the motion of the polymer chain from thermodynamic non-equilibrium state to the thermodynamic equilibrium state.

It is well known that PTT is not an amorphous polymer, because its chain can rearrange to crystallize during non-isothermal process and this phenomenon is concerned with cohesive entanglements along the chains. It is believed that sufficient rearrangement time is a necessary prerequisite to form new cohesive entanglements along the chains when rapidly quenching PTT from the melt state to a temperature below the glass-transition temperature (T_g). As a result, the inter-chain cohesive entanglement is frozen below T_g , which is a usual topological entanglement. The gauche conformation is mainly present in amorphous PTT.^{20, 21} In addition, previous studies found that formation of microphase separation by spinodal decomposition was caused by orientation fluctuations of rigid segments prior to crystal nucleation.^{22, 23} Accordingly, crystallization of PPT film starts when the temperature is up to 56 °C , and the temperature region from 56 °C to 60 °C corresponds to the induction phase during crystallization (I) (Figure 2(b)) due to the parallel arrangement of chains dominating the molecular chain motion and structure.²³

As temperature rises further, the molecular chain entanglement cohesion plays a leading role, and a kind of binary or multiple inter-chain cohesion with local parallel alignment of the neighboring chain segments is formed by the van der Waals' force. Note that the trans conformation related to extensive molecular chains presents in both the crystalline and the amorphous regions, while gauche conformation corresponding to curling molecular chains only presents in the amorphous region. When being treated at temperatures above T_g , both disentanglement of inter-chain cohesive entanglements and parallel arrangement of local chain segments take place, which accelerates the conformation of the molecule chain from gauche to convert trans conformers. It is interesting that the trans conformers are in favor of binary or multiple inter-chain cohesion formation. Then, the amount and size of the parallel-arranged structures increase until a critical size is reached. Thus the nuclei form and crystallization starts (N, 60 °C – 62 °C). The recombinant arrangement of polymer chains leads to Raman intensity decreasing during the crystallization process.

After the nucleation process, the Raman intensity increases rapidly with an increase in temperature because of extremely fast growth of the crystal. This enhanced scattering intensity probably results from a greater volume of the crystal region present in PTT film at elevated temperature. The temperature region from 56 °C – 60 °C is known as the nucleus growth phase (NG, 62 °C – 70 °C). Both the nucleation phase and the nucleus growth phase are called primary crystallization (C_p).

The volume of the crystal region gradually reaches the maximum as the temperature increases to 70 °C . This inflexion point can be regarded as a critical temperature, in that impingement of spherical stacks may locally occur during the primary crystallization. Therefore, the characteristic

temperature of secondary crystallization is 70 °C , and the process above 70 °C is named secondary crystallization (C_s).²⁴ This suggests that the secondary crystals growing in the inter-spherical stacks in the amorphous phase may act as the physical cross-links, which slows down segmental dynamics and gives a gentle increase of the volume of spherical crystals.¹⁰

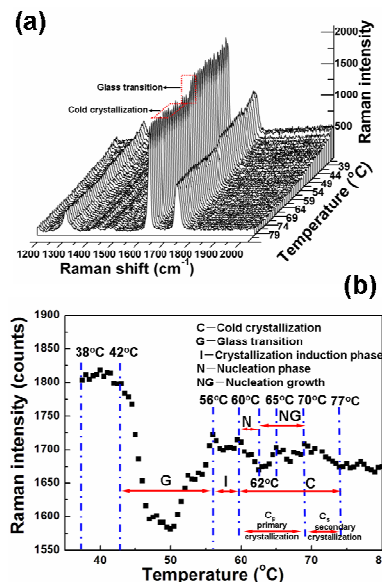


Figure 2 (a) Typical Raman spectra of an amorphous PTT film at a certain temperature. (b) Raman intensity of an amorphous PTT film at 1616 cm^{-1} with a function of temperature (the heating rate is 5 °C/min in nitrogen).

The above results demonstrate that both glass transition and cold crystallization of an amorphous PTT film are exactly detected by Raman technique, in accord with DSC and infrared spectroscopy methods (Figure S1). Moreover, the Raman technique is able to offer more detailed information about the non-isothermal heating process. A model is proposed to depict the entire structural evolution of PTT chains during the non-isothermal crystallization (Figure 3), and the movement of molecular chain and structural evolution of PTT are monitored by the Raman spectrum (Figure 4).

It can be seen that when the PPT film is being treated at temperatures above T_g , both parallel arrangement of local chain segments and disentanglement of inter-chain cohesive entanglements take place, which makes the scattering frequency of C=O invariable in the temperature region from 56 °C – 60 °C (process I to II, Figure 4 (b)). As temperature raises further, the amount and size of the parallel-arranged structure increase, which leads to nuclei formation and crystallization initialization (N, $60\text{ °C} < T < 62\text{ °C}$). In this process, the drastically parallel arrangement of local chain segments takes place and inter-chain cohesive entanglement is the main motion. Synchronously, the scattering frequency of C=O blue-shifted to a low wavenumber because the conformation of PTT molecule changes from gauche to trans conformers (process II to III, Figure 4 (b)). When the crystal nucleus grows further, the adjacent molecular chains are being oriented in parallel with each other to form a large amount of sheaflike crystals, which leads that the scattering frequency of C=O blue-shifted to a low wavenumber (NG: $62\text{ °C} < T < 65\text{ °C}$,

process III to IV). Those sheaf-like crystals probably act as junction points to facilitate aggregate structure growth. This process is known as the nucleus growth phase.³ When the spherical crystallites are formed, based on sheaf-like crystals, the physical interaction between polymer chains can be neglected, and scattering frequency of C=O is invariable in the temperature region from 65 °C to 70 °C (process IV to V). As crystallization time is further prolonged, the secondary crystallization starts, and the aggregation or propagation of spherical crystallites takes place, resulting in the formation of gigantic spherical crystal clusters in the temperature region from 70 °C–77 °C (see the insert of Figure 4(b), process V to VI). In this process, the scattering frequency of C=O is reduced by strong dipole-dipole interaction of the C=O bond during secondary crystallization.^{25,26}

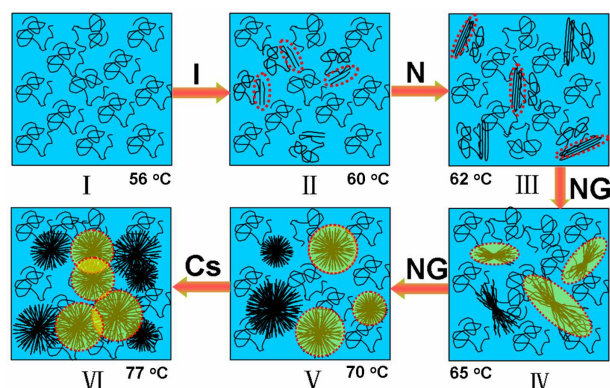


Figure 3 Movement of molecular chains and structure evolution of cold-crystallized PTT. I: crystallization induction phase, N: nucleation phase, NG: nucleus growth phase, Cs: secondary crystallization phase.

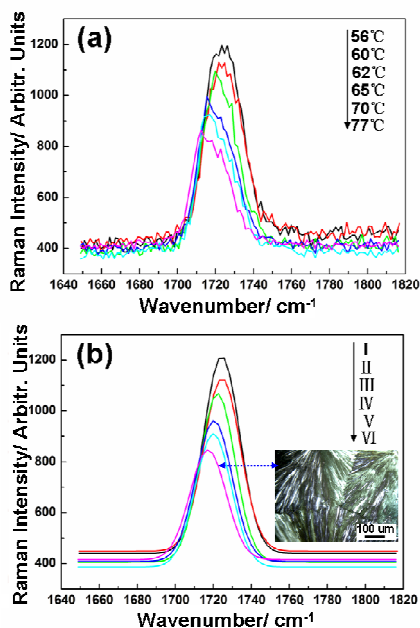


Figure 4 (a) The Raman spectra of the C=O stretching vibration for amorphous PTT film at 56 °C, 60 °C, 62 °C, 65 °C, 70 °C and 77 °C. (b) Gaussian fitting analysis of the C=O stretching vibration.

Isothermal cold crystallization kinetics

Based on the above discussion, the molecular chain motion and microstructure development of PTT amorphous film is facily inspected by Raman spectroscopy under non-isothermal heating conditions. In fact, the structural evolution of chains from a fully amorphous state under isothermal conditions can also be detected by time-resolved Raman spectrum. The scattering intensity of the band at 1616 cm⁻¹ (ring stretching) depends on different isothermal crystallization temperatures, as shown in Figure S2. It can be seen that the crystallization process is related to the scattering intensity of band at 1616 cm⁻¹. The scattering intensity decreases with increasing of the crystallization, until the whole crystalline procedure completed. Therefore, the simplest two-phase model (amorphous and crystallization phases) is assumed in the present Raman scattering system. We can describe the Raman scattering of the semi-crystalline state in terms of crystallinity fraction, X , and write the total scattering, I , by²⁷:

$$I = (1 - X_t) \times I_a + X_t \times I_c \quad (1)$$

where X_t is the crystallinity of PTT film, I_a and I_c are the scattering intensities of amorphous and crystallized PTT, respectively. It can be assumed that the local conformation of amorphous film is unaffected by the crystallization due to the absolute isotropic state in the amorphous phase, so its scattering intensity can be described as a constant (I_0), and the relative crystallinity of PTT film during the cold crystallization can be defined by:²⁸

$$X_t = \frac{X_c(t)}{X_c(t=\infty)} = \frac{I_\infty - I_t}{I_\infty - I_0} \times 100\% \quad (2)$$

Here X_t is the relative crystallinity at time t ; I_t and I_0 are scattering intensities at time t and at the beginning, respectively; I_∞ is the maximum Raman scattering intensity during the crystallization.

To better understand the structural variation during isothermal cold crystallization of amorphous PTT, the relative crystallinities dependant on crystallization time at different temperatures are drawn in Figure 5(a), produced from the Figure S2 and eqn (2). It is known that the common approach for describing the isothermal crystallization kinetics is the Avrami model:²⁸

$$\log[-\ln(1 - X_t)] = \log K + n \log t \quad (3)$$

where K and n stand for rate constant and the Avrami exponent, respectively. K and n depend on nucleation and growth mechanisms of spherulites, which can be obtained from the linear regression curve of $\log[-\ln(1 - X_t)] \sim \log t$. Figure 5(b) shows the Avrami plots of amorphous PTT film isothermally cold-crystallized at different temperatures measured by the Raman spectroscopy. The kinetic parameters are listed in Table 1.

It can be seen that the Avrami exponents obtained by the Raman technique are around 1.05–1.41, suggesting the outward growth of sheaf-like stacks prior to impingement due to a 2D crystal development during cold-crystallization. With the rapid growth of the sheaf-like crystallite, the subsequently interconnected networks would be eventually linked into 3D networks to from a spherical structure during the secondary crystallization.²⁹ Moreover, the results are similar to those obtained by fluorescence spectroscopy (1.05–2.21), resonance

light scattering technique (1.64–1.98)¹⁰ and DSC (1.53–2.38).³ Clearly, the Raman technique is accurately proportional to study the structure evolution and crystallization kinetics of PPT film. Also, the activation energy is estimated at 242.26 kJ mol⁻¹ based on the Arrhenius equation ($k = A\exp(-E/RT)$) by the Raman technique. The high value of activation energy reveals that a plenty of PTT monomer units must be rearranged during cold-crystallization.

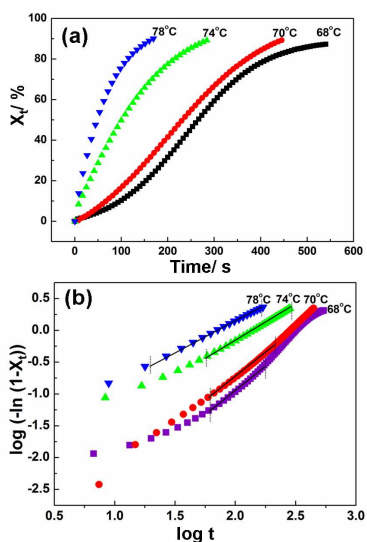


Figure 5 (a) Dependence of relative crystallinity on crystallization time of cold-crystallized PTT at different temperatures obtained by the Raman technique. (b) Avrami plots of isothermally cold-crystallized PTT measured by the Raman technique.

Table 1 Avrami crystallization kinetics parameters of cold-crystallized amorphous PTT determined by the Raman technique.

| T/°C | n | K/min ⁻ⁿ | ΔE/kJmol ⁻¹ |
|------|------|----------------------|------------------------|
| 68 | 1.41 | 1.78×10 ³ | 242.26 |
| 70 | 1.35 | 3.85×10 ³ | |
| 74 | 1.12 | 3.56×10 ² | |
| 78 | 1.05 | 4.85×10 ² | |

Conclusions

In summary, the results obtained by the Raman technique method are in good agreement with those obtained by the IR and DSC method. As an evaluation of the performance of the Raman spectroscopy method, interpretability of the spectral changes taking place in the cold-crystallization process of PTT is investigated in relation to time-dependent structural evolution. This study proves that the Raman spectroscopy technique is a suitable tool for investigating the dynamic crystallization process of polymers. In particular, it is helpful for the studies on the dynamics of energy and electron transfer in chromophore arrays. The blue-shifted quality of C=O stretching vibration resulting from the crystallization

process is a popular phenomenon, and it may have many potential applications in a wide range of areas.

Acknowledgements

Dr. C. L. Hu gratefully acknowledged the support of the Natural Science Foundation of China (Grant NO. 51303066). Prof. X. Chen and J. Chen acknowledged the support of the Natural Science Foundation of China (Grant No. 51233008 and 51373205).

Notes and references

- J. Wu, J. M. Schultz, J. M. Samon, A. B. Pangelinan, H. H. Chuah. *Polymer*, 2001, 42, 7141–7151.
- S. J. Bai, R. J. Spry, M. D. A. Jr, J. R. Barkley. *J. Appl. Phys.*, 1996, 79, 9326.
- W. A. Luo, Z. Z. Liao, J. Yan, Y. Li, X. D. Chen, K. C. Mai, M. Q. Zhang. *Macromolecules*, 2008, 41, 7513–18.
- I. J. Desborough, I. H. Hall, J. Z. Neisser. *Polymer*, 1979, 20, 545–552.
- S. Poulin-Dandurand, S. Perez, J. F. Revol, F. Brisse. *Polymer* 1979, 20, 419–426.
- R. Jakeways, I. M. Ward, M. A. Wilding, I. J. Desborough, M. G. Pass. *J. Polym. Sci. Polym. Phys.*, 1975, 13, 799–813.
- S. Frisk, I. R. M. keda, D. B. Chase, A. Kennedy, J. F. Rabolt. *Macromolecules*, 2004, 37, 6027–6036.
- W. A. Luo, Y. J. Chen, X. D. Chen, K. C. Mai, M. Q. Zhang. *Macromolecules*, 2008, 41, 3912–3918.
- P. D. Honga, W. T. Chuanga, W. J. Yeha, T. L. Lin. *Polymer*, 2002, 43, 6879–6886.
- W. A. Luo, X. D. Chen, Z. F. Liao, J. Yang, K. C. Mai, M. Q. Zhang. *Phys. Chem. Chem. Phys.* 2010, 12, 4686–4693.
- Chum H. *Polym. Eng. Sci.*, 2001, 41, 308–313.
- A. Sanz, A. Nogales, T. A. Ezquerra, M. Soccio, A. Munari, N. Lotti. *Macromolecules*, 2010, 43, 671–679.
- W. T. Chuang, W. B. Su, U. S. Jeng, P. D. Hong, C. J. Su, C. H. Su, Y. C. Huang, K. F. Laio, A. C. Su. *Macromolecules*, 2011, 44, 1140–1148.
- D. A. Ivanov, G. Bar, M. Dosiere, M. H. J. Koch. *Macromolecules*, 2008, 41, 224–9233.
- Z. Yin, C. Koulic, C. Pagnouille, R. Jérôme. *Langmuir*, 2003, 19, 453–457.
- G. Ellis, F. Román, C. Marco, M. A. Gómez, J. G. Fatou. *Spectrochimica. Acta. Part. A*, 1995, 51, 2139–2145.
- X. J. He, H. H. Chuah, M. S. Ellison. *Polym. Bull.*, 2004, 51, 285–291.
- P. D. Olmsted, W. C. K. Poon, T. C. B. McLeish, N. J. Terrill, A. J. Ryan. *Phys. Rev. Lett.*, 1998, 81, 373.
- L. J. Fina, D. I. Bower, I. M. Ward. *Polymer*, 1988, 29, 2146–2151.
- R. Y. Qian. *Macromol. Symp.* 1997, 124, 15–16.
- R. Y. Qian, D. Y. Shen, F. G. Sun. *Macromol. Chem. Phys.*, 1996, 197, 1485–1493.
- M. Imai, K. Kaji, T. Kanaya. *Phys. Rev. Lett.* 1993, 71, 4162.
- W. T. Chuang, P. D. Hong, K. S. Shih. *Polymer*, 2004, 45, 8583–8592.
- C. Alvarez, I. Šicsa, A. Nogales, Z. Dencheva, S. S. Funarib, T. A. Ezquerra. *Polymer*, 2004, 45, 3953–3959.
- S. S. Jang, W. H. Jo. *Macromolecules*, 2001, 34, 6985–6993.
- H. H. Chuah. *Macromolecules*, 2011, 34, 6985–6993.
- Y. Xu, H. B. Jia, J. N. Piao, S. R. Ye, J. Huang. *J. Mater. Sci.*, 2008, 43, 417–421.
- M. Avrami. *J. Chem. Phys.* 1940, 8, 212.
- N. Vasanthan, S. Ozkaya, M. Yaman. *J. Phys. Chem. B*, 2010, 114, 13069–13075.